Hindawi Publishing Corporation
Journal of Nanomaterials
Volume 2011, Article ID 910962, 8 pages
doi:10.1155/2011/910962

Research Article

Constitutive Rheological Modeling of Flow Serration Behaviour in Metallic Glasses Showing Nanocrystallization during Deformation

M. A. Yousfi,[1] K. Hajlaoui,[2,3] Z. Tourki,[1] and A. R. Yavari[3]

[1] *LMMP LAB-STI03, Université de Tunis, ESSTT, Tunis 1008, Tunisia*
[2] *LGM-MA05, ENIM, Av. Ibn El Jazzar, Monastir 5019, Tunisia*
[3] *SIMaP-LTPCM, Institut National Polytechnique de Grenoble, 38402 Saint Martin d'Heres, France*

Correspondence should be addressed to K. Hajlaoui, k.hajlaoui@yahoo.fr

Received 25 April 2010; Revised 26 June 2010; Accepted 16 July 2010

Academic Editor: Quanqin Dai

A simple micromechanism-inspired rheological model is developed that incorporates the serrated flow nature of metallic glasses subjected to compressive deformation at room temperatures. The process of propagation and the arrest of shear bands were addressed in this model. Shear-induced nanocrystallisation was believed to be responsible for strain hardening of material within the shear bands. The model is based on the assumption that the behaviour can be decomposed into two resistances acting in parallel: one captures the initial stiffness and shear softening and the second gives the time-shear-temperature hardening of material.

1. Introduction

Metallic Glasses (MGs) (amorphous metals) are a new class of engineering materials which have attracted large technological interests [1–5] and are finding increased use as functional materials in the sporting goods, MEMS (Micro-Electro-Mechanical Systems) and NEMS (Nano-Electro-Mechanical Systems). The first metallic glass system was developed by Klement et al. [6] which consisted of a binary Au–Si alloy. At present, some of the most commonly researched metallic glasses include the Zr-based, Pd-based, Cu-based, and many other alloy systems. These amorphous alloys are produced by the rapid quenching of liquid metals from a molten state to prevent crystallization. Hence, metallic glasses can be considered as nanocrystalline material with ultimate reduction in grain size (in the order of a few nanometers). It has an amorphous structure (structure less), and it is void of dislocations and defects which weaken conventional crystalline alloys. Consequently, MGs possess excellent mechanical properties [7–9], practical physical properties, and unique chemical properties (good corrosion resistance) [10], as well as great potential for structural and functional applications. While many MGs have demonstrated the highest specific strengths and showed considerable fracture toughness, their deformation mechanisms are basically different from those of crystalline solids due to their lack of long-range atomic order. Usually it is understood that under room temperature and uniaxial stress states, MGs deform through a procedure of highly localized shearing in narrow bands that are thin layers of material being initially only 10 nm thick [11] and fail along one dominant shear band catastrophically [12]. The macroscopic fragility severely limits further exploitation of this class of advanced materials. However, in some cases, values of more than 50% of plastic deformation have been achieved [13] in some monolithic metallic glasses. During deformation, structural changes possibly occur within the shear bands. Several experimental evidences for deformation-induced nanocrystallization in shear bands have been reported in our previous work [14–16] based on transmission electron microscopy (TEM) study. A high plastic strain has been also reported, for example, in Pd-based MG [17] where the authors attribute this result to a nanoscale phase separation which blocks the propagation of shear bands facilitating

their initiation and branching. All MG systems exhibiting large plasticity deform via formation of numerous shear bands all over the compressed specimen, and the degree of the plasticity is predominantly dependent on the total number of shear bands generated during deformation. These "ductile" MGs have generally the characteristic deformation features that are serrated flow, that is, elastically loading and plastically unloading with sharp stress drop, in stress-strain curves. Furthermore, currently, it is accepted that the macroscopic serrated plastic flow behaviour is associated with the shear-banding process on a nanoscale within MGs, and extensive efforts have been made to bare the relationship between them.

As metallic glasses lack crystalline order, and therefore structural features such as dislocations and grain boundaries, the application of conventional metallurgical theory is generally not allowed. As such, significant efforts to develop suitable mechanistic models for the description of mechanical behaviour continue in order to best capture the principal feature of MGs. A constitutive equation accounting for the presence of serrated flow as kinetic phenomenon of plastic deformation in MGs is presented in the present work in light of the recent microscopic findings. Deformation-induced nanocrystal formation in the shear band regions will be highlighted, and the effect of this phenomenon on the arrest of shear bands will be analysed and modeled.

2. Aspect of Experimentally Observed Stress-Strain Behaviour

The typical stress-strain behaviour of Metallic Glass at room temperatures is shown in Figure 1. The tested Bulk Metallic Glass (BMG) of compositions $Zr_{55}Al_{10}Cu_{20}Ni_{10}Pd_5$ was prepared by arc melting the pure elements under Ti-gettered Ar atmosphere followed by casting into a water-cooled copper mould. The resulted ingots were bars with dimensions 2 mm × 4 mm × 75 mm. Compression test specimens with dimensions of 2 mm × 2 mm × 4 mm (aspect ratio 2 : 1) were cut from the BMGs. The outer surfaces of the specimens, especially the ends in contact with the cross-head, were mechanically polished to ensure flat and parallel surfaces. Compression tests were conducted at constant strain rate of $8 \times 10^{-4}\,s^{-1}$ using a Schenck hydraulic testing machine at room temperature. The yield stress is measured to be 1800 MPa, and the maximum plastic strain is 4.7%. The overall plastic deformation is accomplished by serrated flow process. As highlighted by the insert in Figure 1, the "unit" of the plastic flow serrations consists of elastic loading portion followed by a sudden load drop and displacement burst. The amplitude of the stress drops gradually increases with strain, and the slopes of both loading and unloading of the serrations are nearly constant from the yield point to the ultimate failure. The slope of the unloading sections is linked with the inelastic displacements produced by local shear deformation with rapid stress drops.

Recent experiments show that the load serrations are related to the intermittent propagation of individual shear bands [18, 19] which results from the interaction between the

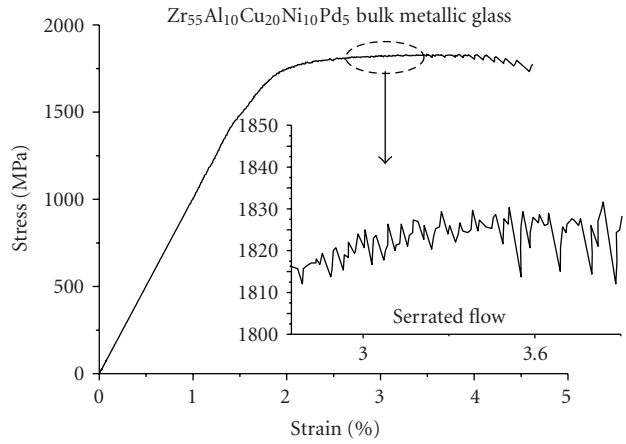

Figure 1: A representative compression stress-strain curve of the $Zr_{55}Al_{10}Cu_{20}Ni_{10}Pd_5$ Bulk Metallic Glass deformed at room temperature and for strain rate of $8 \cdot 10^{-4}\,s^{-1}$. The inset shows the magnified view in the serrated flow region.

processes of shear-induced materials softening and structural relaxation [19, 20]. More recently, Chen et al. [21], using in-situ TEM deformation experiments, showed that even for very small size samples, the load-displacement curve indicates occurrence of multiple shear bands, and none of these shear bands run over a long distance upon initiation. They are arrested after a small distance of propagation (20 nm).

The repeated arrest and reactivation of shear bands have not been explained convincingly, and none of the proposed constitutive equations for inhomogeneous plastic flow deal with the serrated flow adequately. It seems that the arrest mechanism that effectively stops the runaway slip along a single shear band plays a significant role in the plasticity of the monolithic BMGs. Thus, the suitable model must include details on micromechanisms of the serrated flow, in particular the arrest of shear bands.

For this reason, the deformed sample was carefully cut along a plane perpendicular to the shear bands and characterized by TEM. Foils preparation and experimental details were well developed in our previous work [14–16]. The dark field image and the broad halo SAED (selected area electron diffraction) obtained from the deformed Zr-based Bulk MG are presented in Figure 2. This figure shows typical white contrast of shear bands surrounded by amorphous regions. Nanocrystals with a size of around 10 nm are distributed within the shear band and cannot be found in the regions out of the band, suggesting that their formation is associated with the localized shear deformation. The nanocrystallization within shear bands can be further confirmed by the fine diffraction rings (see arrow in Figure 2) observed by nanobeam electron diffraction.

Remarkably, as evidenced by TEM imaging, the nanocrystallization from the amorphous phases investigated in this work already occurs during the first stage of deformation due to convinced mechanical activation energy. This phenomenon is well known as the deformation-induced nanocrystallization in metallic glasses and has

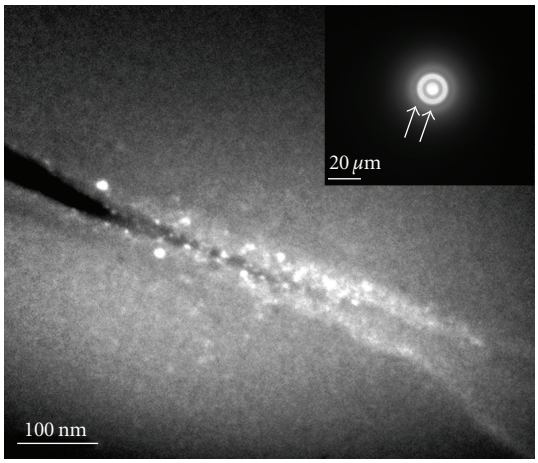

Figure 2: TEM dark field micrograph of shear band (followed by cracks propagation) in the uniaxially deformed $Zr_{55}Al_{10}Cu_{20}Ni_{10}Pd_5$ Bulk Metallic Glass showing the presence of nanocrystallites with an average size of 10 nm embedded in the amorphous matrix. Inset is the corresponding selected area electron diffraction (SAED) pattern recorded from the regions within the shear band.

been observed in a number of MGs with large plastic deformation [22–24]. Theses studies have demonstrated that nanocrystallites play an important role in increasing the plasticity of amorphous metallic alloys by retarding sudden shear bands propagation. Likewise, the nanocrystallization during shear flow can offer a "self-locking effect" to avoid further propagation of shear bands. Therefore, the influence of the insitu nanocrystallization on the mechanical behaviour of MGs remains to be comprehensively clarified and parameters involving the mechanism of deformation-induced nanocrystallization must be included somewhat in constitutive model for plastic deformation of metallic glasses.

3. Constitutive Model: Background and Development

The experimental data presented in the previous section clearly show the complicated behaviour that is exhibited by MGs, particularly the correlation between the yields drops in the load-displacement curve and the nature of dynamic emission and propagation of shear bands. There are obviously two possibilities; the first is that each yield drop step corresponds to the formation of a new shear band the second is that the yield drops are due to intermittent slip on existing shear bands. In Fact, when the propagation of shear band is suddenly suppressed by the disappearance of the confined viscous flow, which results in the nanocrystals formation, then, the other shear band will start to move in the amorphous glassy structure close to the region where the previous shear band was arrested. Repeating the process during deformation, a large plasticity can be obtained by potential shear band branching.

To address these observations, a simple micromechanism inspired model is developed that incorporates the serrated flow nature of deformed material. We will limit this work to highlighting the individual shear striation behaviour under the assumption that each serration is associated with individual shear events. In this section, we describe the details of the microscopic mechanism steps, which we believe is occurring in a very narrow shear zone during deformation in MGs (see Figure 3). Each step will be modelled separately. The development of a physically based constitutive model for the stress-strain behaviour of MGs can now begin with an interpretation of the data discussed previously and schematically presented in Figure 3. The model is interpreted below in terms of a series of two conceptual steps.

Step 1 (initial dilatation and shear softening). The initial portion of the stress-strain curve displays a stiff response followed by stress drop (see Figure 3(a)). Initial deformation in this step is accompanied by significant shear-induced dilatation of the structure. The strain can be promptly accommodated at the atomic level through variations in neighbourhood, atomic bonds. The exact nature of local atomic motion in straining MGs is not fully determined, although there is general agreement that the basic unit process underlying deformation should be local atoms rearrangement that can accommodate shear strain as schematically shown in Figure 3(b). An equivalent of this local rearrangement is illustrated in the two-dimensional schematic originally proposed by Argon [25] and usually known as "shear transformation zone" (STZ) [25–28] which is basically a local cluster of atoms that endures an inelastic shear distortion.

An alternative, complementary viewpoint on this mechanism is given by the classical "free-volume" model, firstly developed by Turnbull and Cohen [29–31] and applied by Spaepen [32] to the case of MGs deformation. This model considers deformation as sequences of discrete atomic jumps in the metallic glass, as implicitly depicted in Figure 3(b). These mechanisms (whether one subscribes to an STZ-type or diffusive-like jump mechanism) may occur homogeneously over a glass body (for example at high temperatures) [33, 34], or in a localized mode as throughout the formation of a shear band (at room temperature) as the case of the present work where the constitutive model will correspond to what most likely happen in individual shear bands. These microscopic models have been widely used to review the basic features of metallic glass deformation [35–38] as well as the kinetics of structural relaxation of these materials [39, 40]. The equations derived from these models well capture the transition from linear elastic dilatation to stress drop due to shear softening.

We shall then recall these dilatation models for the first step of stress-strain curve. According to Spaepen [32], microscopic flow is occurring as a result of a number of individual atom jumps, each participating to a slight local shear strain. This process occurs at sites where large enough holes or flow defects, with a size larger than a critical value making an atomic diffusive jump possible. The plastic strain rate is given as follows [32]:

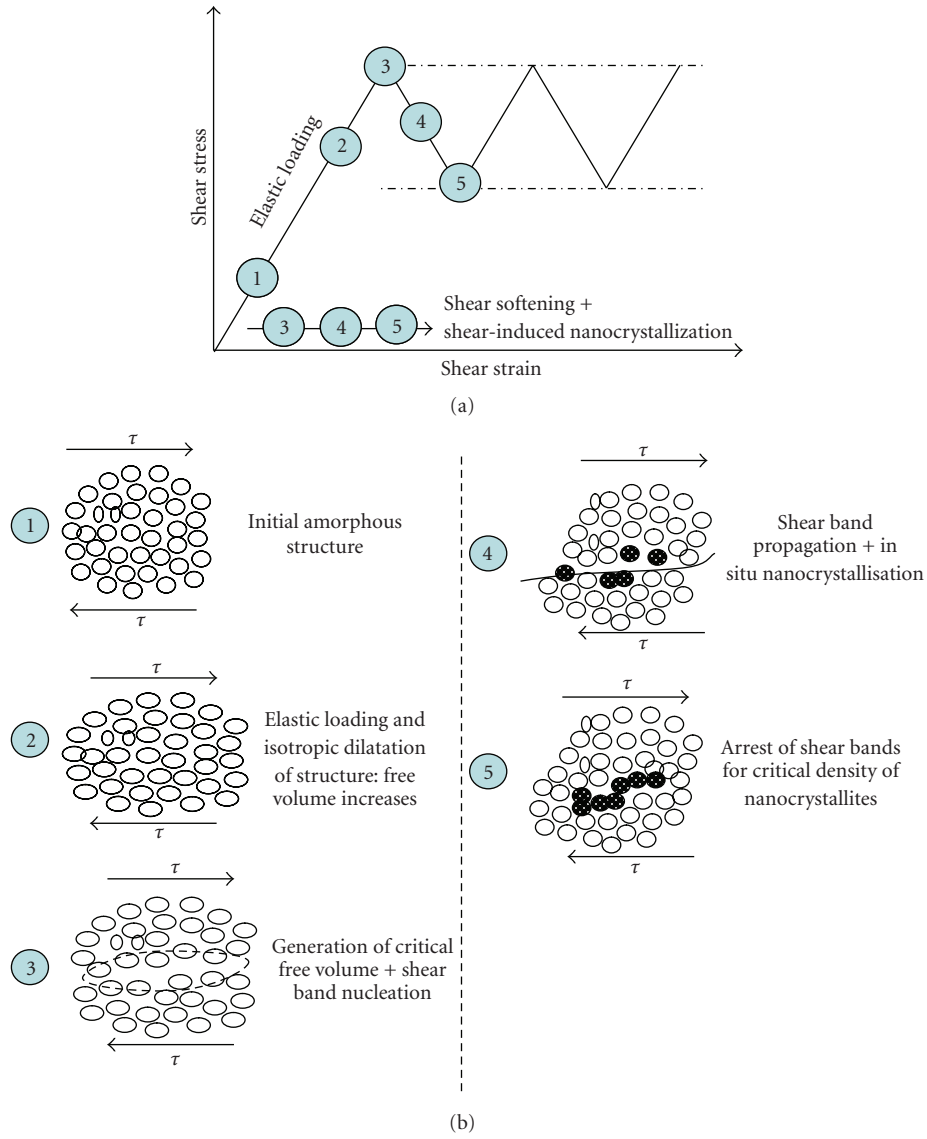

Figure 3: (a) Schematic illustration showing the details of the proposed model for serrated flow in metallic glasses. (b) The corresponding atomic illustrations of propagation of individual shear band in nanoscale range: (1)-(2) elastic deformation through conventional structural dilatation mechanism, (3)-(4) free volume creation and shear band propagation at initial stage going with structural segregation and nanocrystallization by concentration of shear stress, (5) suppression of propagation and arrest of shear band by precipitation and growth of nanocrystalline particles within the shear zone.

$(\partial\gamma/\partial t)$ = (strain produced at each site) × (fraction of potential jump sites) × (net number of forward jumps at each site per second).

Within the free-volume formalism, $\partial\gamma/\partial t$ can be written as [32]

$$\frac{\partial\gamma}{\partial t} = 2 \cdot \mathrm{f} \cdot C_f \cdot \exp\left[-\frac{\Delta G^m}{k_B \cdot T}\right] \sinh\left(\frac{\tau \cdot \Omega}{2 \cdot k_B \cdot T}\right), \quad (1)$$

where ΔG^m is the activation energy for an atomic jump; f is the jump frequency; T is the temperature, k_B is the Boltzmann's constant; Ω is the atomic volume; $C_f = \exp(-\gamma v^*/v_f)$ is the concentration of the flow defects. It relates to the so-called reduced free volume $v_f/\gamma v^*$ according to [29] and where γv^* is approximated as 0.5 Ω [41], and v_f is the mean free volume per atom.

The softening observed in stress-strain curves of Figure 3(a) can be justified by several potential causes involving the local creation of flow defects due to flow dilatation [42–45], the local evolution of structural order [46, 47] and the local heat generation [48–50]. Due to these causes, viscosity can decrease dramatically according to the so-called "hybrid" equation [51]:

$$\eta_s\left(T, C_f\right) = \eta_0 \cdot \exp\left(\frac{Q_n}{R \cdot T}\right)\left(\frac{1}{C_f}\right), \quad (2)$$

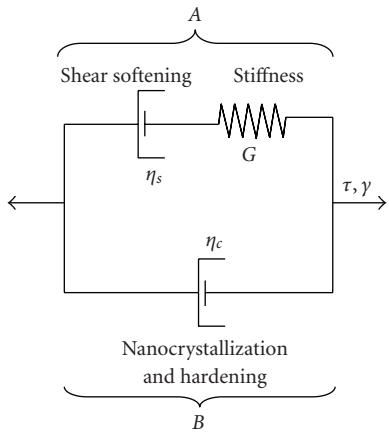

FIGURE 4: Schematic representation of rheological model for mechanical behaviour of individual shear band in light of experimental results (Figure 1) and the proposed micromechanism of deformation in metallic glasses (Figure 3). Interatomic resistance (stiffness) is followed by shear softening (η_s), acting in parallel with hardening induced by in situ nanocrystallization (η_c).

where η_0 is a pre-exponential factor Q_n is the activation energy for viscous flow.

The change in the defect concentration C_f can be estimated as a balance between structural relaxation and strain-induced nucleation. This leads to the general equation [52]

$$\frac{dC_f}{dt} = -k \cdot C_f \cdot \left(C_f - C_{f,\mathrm{eq}}\right) + a \cdot \dot{\varepsilon} \cdot C_f \cdot \left(\ln C_f\right)^2. \quad (3)$$

k is a temperature-dependent rate factor for structural relaxation, which has the form of $k = k_0 \exp(-E_r/RT)$ with k_0 being the attempt frequency and E_r being the activation energy for relaxation a is a proportionality factor. $C_{f,\mathrm{eq}}$ denotes the defect concentration in the metastable equilibrium state [51]

Now, we go back to the proposed rheological model of Figure 4, and according to the described microscopic mechanism of deformation, the initial linear dilatation is modeled with a three-dimensional linear elastic spring acting in series with a viscous element denoting the softening part ($\eta_s(C_f, T)$). The spring represents the initially stiff elastic response due to interatomic bonds in material, and the viscosity is taken to be initial as for metallic glasses (η_0) and is temperature-straindependent according to (2). Once the stress reaches a critical level, critical concentration of defect is overcome, viscosity decreases, and shear flow softening follows. The deformation can therefore be decomposed into elastic and plastic flows with stress softening.

Step 2 (Strain Hardening and Arrest of Shear Band Propagation). The Arrest of the shear bands has not been well understood and is still the matter of debate. Chen et al. [53] showed that a propagating shear band initially accelerates and then reaches a steady state, and finally the propagating shear band decelerates and is arrested. This indicates that a mechanism of the blocking in a shear band is operating, which is a significantly important issue, and it is worthy of progressive study.

Several factors have been suggested to cause the arrest of the shear bands. Recently, Dalla Torre et al. [19] suggested that structural relaxation can occur after a shear event going with the annihilation of strain-created free volume, and therefore it causes a time-dependent hardening in the vicinity of the shear band. Alternatively, deformation-induced nanocrystallization observed in our previous work [14–16] and confirmed in a number of MGs showing large plastic deformation provides a potential reason for the strain-hardening mechanism. The presence of nanocrystallites in shear bands has a direct effect on viscosity, increasing its value with increasing the content of particles. As suggested in our previous work, shear bands can act as semisolid MG slurries since, as discussed in step 1, shear in metallic glasses generates free volume and heat, reduces viscosity, and leads to liquid-like behaviour in the shear bands with a possible rise in temperature. Under these conditions, the increase of the amount of nanocrystals in the shear zone can dramatically increase viscosity according to the correlation between viscosity and the fraction of nanocrystal solids (for semisolid behaviour) [54–56]

$$\eta_c(\gamma, \dot{\gamma}, T) = \eta_l \cdot \left(1 - \frac{\phi_s(\gamma, \dot{\gamma}, T)}{\phi_{\mathrm{cr}}}\right)^{-\alpha}, \quad (4)$$

where η_c is the increased viscosity of the flowing system of liquid and solids (nanoparticles) η_l is the viscosity of the liquid ϕ_s is the solid fraction of the suspension α is a constant, ϕ_{cr} is a critical value of particle fraction beyond which the relationship no longer holds since the system becomes jammed $(0,5 < \phi_{\mathrm{cr}} < 0,6)$.

The nanocrystallization is a rate-dependent function of shear deformation along shear bands, and the fraction of the crystalline phase increases with shear strains. Therefore, the arrest of shear strain corresponds to a critical value of volume fraction of the crystalline particles (or nanocrystalline) at which the increased viscosity by the nanocrystallization (and subsequent growth) is high enough to prevent the further shearing along the band. This strengthening caused by in situ nanocrystallization can compensate the strainsoftening ((3)-(4)-(5) steps in Figure 3) and thus prevent the runaway failure along the shear band. Consequently, shear process stops, and system (sample and stiff machine) turns into the elastic form until the creation of a new shear band with further loading (serration behaviour as shown in Figure 1)

The new strain-hardening mechanism acting in parallel with the strain-softening one is modeled with a viscous element where the viscosity η_c is given by (4).

In the end of this phenomenological description of stress-strain behaviour of MGs, it is necessary to address the modeling of flow-induced crystallization. While numerous works showed deformation-induced nanocrystallization during deformation, as of yet, no consensus concerning the microscopic mechanism of mechanically-induced nanocrystallization has been achieved. Recent investigations [57–60], based on TEM observations, have proposed a model for nanocrystallization mechanism in the BMGs. Since

amorphous alloys are not in thermodynamic equilibrium, a phase transformation from an amorphous liquid-like phase to a crystalline phase can take place with the supply of sufficient external energy. Thermal energy [57, 61] and mechanical energy [58, 59] are two major driving forces controlling this transformation as well as the assistance of the local atomic rearrangements in the shear band [60].

Actually, since the amorphous crystal transformation in shear bands is a new phenomenon and not fundamentally addressed, we shall use it for the first assumption of the classical theory of crystallization applied for metallic glasses. Crystallization of an amorphous liquid can be regarded as process taking place by crystal nucleation and subsequent growth. During the nucleation process, a crystalline embryo is formed in the amorphous liquid, and meantime, the interface is formed simultaneously. The overall rate of transformation will reflect the time, temperature, shear, shear rate, and so forth dependence of both nucleation and growth process. This is usually described by the Johnson-Mehl-Avrami equation [58]

$$\phi_s(\gamma, \dot{\gamma}, T) = 1 - \exp(-b(T) \cdot t^n) \approx 1 - \exp\left(-b(T) \cdot \left(\frac{\gamma}{\dot{\gamma}}\right)^n\right), \tag{5}$$

where $b(T) \approx b_0 \exp(\Delta G^*/RT)$ is a rate constant, and n is an exponent between 1.5 and 4. ΔG^* is the activation energy for overall crystallization process which can be obtained from the thermodynamic point of view of amorphous-to-crystalline phase transformation [24, 59, 60] or from continuous heating experiments using kissinger's [59, 62] or Ozawa's [63] method

$$\Delta G^*(T, P) = \frac{16\pi \cdot \gamma^3}{3} \left(\frac{V_m^C}{\Delta G_m + E_e + P\Delta V_m}\right)^2, \tag{6}$$

where ΔG_m is the molar free energy change for an amorphous-to-crystalline phase transformation; E_e is the elastic energy induced by the volume change upon phase transformation; γ is the interfacial free energy of the crystalline/amorphous interface; V_m^c is the molar volume of the crystalline phase; ΔV_m is the volume change for forming a crystalline nucleus from an amorphous matrix P is the applied hydrostatic pressure. Based on (6), Lee et al. [24] demonstrated that a decrease in activation energy for crystallization can occur within the shear bands due to the increased interface thermal-strain energy and contact pressure-promoted nucleation. Hence, the rapid nucleation of crystals in the shear zone can occur under the high strain rate deformation and adiabatic heating.

4. Mathematical Model Formulation

The mathematical representation of the proposed rheological model is based on the representation of the breakdown of the overall deformation resistance into a resistance A acting in parallel with a resistance B as illustrated in Figure 4. As stated earlier, resistance A come up from interatomic interactions and shear softening where the interatomic interactions are the source of the material's initial stiffness and result in a finite stress at which metallic glasses will plastically soft. In resistance B, hardening by insitu nanocrystallization is a secondary contributor to the shear strain of the material. The two processes (shear softening and material hardening) occur concurrently immediately after the initial stiffness and are therefore modeled as being in parallel after initial elastic strain. The proposed rheological model recognizes that the shear deformation acting on each resistance is equal to the imposed (total) shear deformation γ

$$\gamma = \gamma_A = \gamma_B. \tag{7}$$

The total shear stress τ is the sum of the shear stress acting on each resistance:

$$\tau = \tau_A + \tau_B. \tag{8}$$

We assume that the viscous flow in shear bands is Newtonian, then:

$$\tau_B = \eta_c \cdot \dot{\gamma}_B = \eta_c \cdot \dot{\gamma}, \quad \dot{\gamma} = \frac{\dot{\tau}_A}{G} + \frac{\tau_A}{\eta_s}. \tag{9}$$

For constant shear strain ($\partial\gamma/\partial t$ = constant), (7), (8), and (9) lead to the general relationship between stress and strain resulting in the proposed rheological model for shear-banding behaviour

$$\dot{\tau} = \frac{G}{\eta_s}\left[(\eta_s + \eta_c)\dot{\gamma} - \tau\right]. \tag{10}$$

5. Summary

We conclude our study by a very brief recapitulation of the rheological model that we have proposed. In this paper a new micromechanism-inspired constitutive model has been presented that allows for predictions of single-shear striation behaviour of "ductile" MGs. The model is based on the assumption that the general behaviour can be decomposed into two resistances acting in parallel: one captures the initial stiffness and shear softening, and the second gives the time-shear-temperature hardening of material. The resultant stress-strain curve should be obtained by the resolution of the coupled (1), (3), (4), (5), and (10). Resolution involves a large number of model parameters that must be defined; many of these parameters are fundamental properties of the metallic glasses that can be found in the literature. However, the remaining parameters must be obtained by fitting the above equations to our experimental data and to others recently published data [53, 64]. This is not the aim of this paper, but this study is in progress.

References

[1] A. Peker and W. L. Johnson, "A highly processable metallic glass: $Zr_{41.25}Ti_{13.75}Cu_{12.5}Ni_{10.0}Be_{22.5}$," *Applied Physics Letters*, vol. 63, no. 17, pp. 2342–2344, 1993.

[2] A. Inoue, "Stabilization of metallic supercooled liquid and bulk amorphous alloys," *Acta Materialia*, vol. 48, no. 1, pp. 279–306, 2000.

[3] W. H. Wang, C. Dong, and C. H. Shek, "Bulk metallic glasses," *Materials Science and Engineering R*, vol. 44, no. 2-3, pp. 45–89, 2004.

[4] A. L. Greer, "Metallic glasses," *Science*, vol. 267, no. 5206, pp. 1947–1953, 1995.

[5] W. F. Wu, Y. Li, and C. A. Schuh, "Strength, plasticity and brittleness of bulk metallic glasses under compression: statistical and geometric effects," *Philosophical Magazine*, vol. 88, no. 1, pp. 71–89, 2008.

[6] W. Klement, R. H. Willens, and P. Duwez, "Non-crystalline structure in solidified Gold-Silicon alloys," *Nature*, vol. 187, no. 4740, pp. 869–870, 1960.

[7] A. Inoue, B. Shen, H. Koshiba, H. Kato, and A. R. Yavari, "Cobalt-based bulk glassy alloy with ultrahigh strength and soft magnetic properties," *Nature Materials*, vol. 2, no. 10, pp. 661–663, 2003.

[8] C. J. Gilbert, R. O. Ritchie, and W. L. Johnson, "Fracture toughness and fatigue-crack propagation in a Zr–Ti–Ni–Cu–Be bulk metallic glass," *Applied Physics Letters*, vol. 71, no. 4, pp. 476–478, 1997.

[9] A. R. Yavari, J. J. Lewandowski, and J. Eckert, "Mechanical properties of bulk metallic glasses," *MRS Bulletin*, vol. 32, no. 8, pp. 635–638, 2007.

[10] D. Zander, B. Heisterkamp, and I. Gallino, "Corrosion resistance of Cu–Zr–Al–Y and Zr–Cu–Ni–Al–Nb bulk metallic glasses," *Journal of Alloys and Compounds*, vol. 434-435, pp. 234–236, 2007.

[11] Y. Zhang and A. L. Greer, "Thickness of shear bands in metallic glasses," *Applied Physics Letters*, vol. 89, no. 7, Article ID 071907, 3 pages, 2006.

[12] H. J. Leamy, T. T. Wang, and H. S. Chen, "Plastic flow and fracture of metallic glass," *Metallurgical Transactions*, vol. 3, no. 3, pp. 699–708, 1972.

[13] A. Inoue, W. Zhang, T. Tsurui, A. R. Yavari, and A. L. Greer, "Unusual room-temperature compressive plasticity in nanocrystal-toughened bulk copper-zirconium glass," *Philosophical Magazine Letters*, vol. 85, no. 5, pp. 221–229, 2005.

[14] K. Hajlaoui, A. R. Yavari, B. Doisneau et al., "Shear delocalization and crack blunting of a metallic glass containing nanoparticles: in situ deformation in TEM analysis," *Scripta Materialia*, vol. 54, no. 11, pp. 1829–1834, 2006.

[15] K. Hajlaoui, B. Doisneau, A. R. Yavari et al., "Unusual room temperature ductility of glassy copper-zirconium caused by nanoparticle dispersions that grow during shear," *Materials Science and Engineering A*, vol. 448–451, pp. 105–110, 2007.

[16] K. Hajlaoui, A. R. Yavari, A. LeMoulec et al., "Plasticity induced by nanoparticle dispersions in bulk metallic glasses," *Journal of Non-Crystalline Solids*, vol. 353, no. 3, pp. 327–331, 2007.

[17] K. F. Yao, F. Ruan, Y. Q. Yang, and N. Chen, "Superductile bulk metallic glass," *Applied Physics Letters*, vol. 88, no. 12, Article ID 122106, 2006.

[18] J. C. Ye, J. Lu, Y. Yang, and P. K. Liaw, "Study of the intrinsic ductile to brittle transition mechanism of metallic glasses," *Acta Materialia*, vol. 57, no. 20, pp. 6037–6046, 2009.

[19] F. H. Dalla Torre, A. Dubach, J. Schällibaum, and J. F. Löffler, "Shear striations and deformation kinetics in highly deformed Zr-based bulk metallic glasses," *Acta Materialia*, vol. 56, no. 17, pp. 4635–4646, 2008.

[20] A. Dubach, F. H. Dalla Torre, and J. F. Löffler, "Constitutive model for inhomogeneous flow in bulk metallic glasses," *Acta Materialia*, vol. 57, no. 3, pp. 881–892, 2009.

[21] C. Q. Chen, Y. T. Pei, and J. T. M. De Hosson, "Effects of size on the mechanical response of metallic glasses investigated through in situ TEM bending and compression experiments," *Acta Materialia*, vol. 58, no. 1, pp. 189–200, 2010.

[22] J. B. Qiang, W. Zhang, G. Q. Xie, and A. Inoue, "Unusual room temperature ductility of a Zr-based bulk metallic glass containing nanoparticles," *Applied Physics Letters*, vol. 90, no. 23, Article ID 231907, 2007.

[23] K. Mondal, T. Ohkubo, T. Toyama, Y. Nagai, M. Hasegawa, and K. Hono, "The effect of nanocrystallization and free volume on the room temperature plasticity of Zr-based bulk metallic glasses," *Acta Materialia*, vol. 56, no. 18, pp. 5329–5339, 2008.

[24] S.-W. Lee, M.-Y. Huh, S.-W. Chae, and J.-C. Lee, "Mechanism of the deformation-induced nanocrystallization in a Cu-based bulk amorphous alloy under uniaxial compression," *Scripta Materialia*, vol. 54, no. 8, pp. 1439–1444, 2006.

[25] A. S. Argon, "Plastic deformation in metallic glasses," *Acta Metallurgica*, vol. 27, no. 1, pp. 47–58, 1979.

[26] M. L. Falk, "Molecular-dynamics study of ductile and brittle fracture in model noncrystalline solids," *Physical Review B*, vol. 60, no. 10, pp. 7062–7070, 1999.

[27] A. C. Lund and C. A. Schuh, "Yield surface of a simulated metallic glass," *Acta Materialia*, vol. 51, no. 18, pp. 5399–5411, 2003.

[28] J. S. Langer, "Dynamics of shear-transformation zones in amorphous plasticity: formulation in terms of an effective disorder temperature," *Physical Review E*, vol. 70, no. 4, Article ID 041502, 2004.

[29] D. Turnbull and M. H. Cohen, "Free-volume model of the amorphous phase: glass transition," *The Journal of Chemical Physics*, vol. 34, no. 1, pp. 120–125, 1961.

[30] D. Turnbull and M. H. Cohen, "On the free-volume model of the liquid-glass transition," *The Journal of Chemical Physics*, vol. 52, no. 6, pp. 3038–3041, 1970.

[31] M. H. Cohen and D. Turnbull, "Molecular transport in liquids and glasses," *The Journal of Chemical Physics*, vol. 31, no. 5, pp. 1164–1169, 1959.

[32] F. Spaepen, "A microscopic mechanism for steady state inhomogeneous flow in metallic glasses," *Acta Metallurgica*, vol. 25, no. 4, pp. 407–415, 1977.

[33] K. C. Chan, L. Liu, and J. F. Wang, "Superplastic deformation of $Zr_{55}Cu_{30}Al_{10}Ni_5$ bulk metallic glass in the supercooled liquid region," *Journal of Non-Crystalline Solids*, vol. 353, no. 32–40, pp. 3758–3763, 2007.

[34] G. Wang, J. Shen, J. F. Sun, Z. P. Lu, Z. H. Stachurski, and B. D. Zhou, "Tensile fracture characteristics and deformation behavior of a Zr-based bulk metallic glass at high temperatures," *Intermetallics*, vol. 13, no. 6, pp. 642–648, 2005.

[35] R. Huang, Z. Suo, J. H. Prevost, and W. D. Nix, "Inhomogeneous deformation in metallic glasses," *Journal of the Mechanics and Physics of Solids*, vol. 50, no. 5, pp. 1011–1027, 2002.

[36] M. Bletry, P. Guyot, Y. Bréchet, J. J. Blandin, and J. L. Soubeyroux, "Transient regimes during high-temperature deformation of a bulk metallic glass: a free volume approach," *Acta Materialia*, vol. 55, no. 18, pp. 6331–6337, 2007.

[37] C. A. Schuh, T. C. Hufnagel, and U. Ramamurty, "Mechanical behavior of amorphous alloys," *Acta Materialia*, vol. 55, no. 12, pp. 4067–4109, 2007.

[38] C. A. Schuh and A. C. Lund, "Atomistic basis for the plastic yield criterion of metallic glass," *Nature Materials*, vol. 2, no. 7, pp. 449–452, 2003.

[39] K. Hajlaoui, M. A. Yousfi, Z. Tourki, G. Vaughan, and A. R. Yavari, "On the free volume kinetics during isochronal structural relaxation of Pd-based metallic glass: effect of

temperature and deformation," *Journal of Materials Science*, vol. 45, no. 12, pp. 3344–3349, 2010.

[40] P. A. Duine, J. Sietsma, and A. van den Beukel, "Defect production and annihilation near equilibrium in amorphous $Pd_{40}Ni_{40}P_{20}$ investigated from viscosity data," *Acta Metallurgica Et Materialia*, vol. 40, no. 4, pp. 743–751, 1992.

[41] A. van den Beukel and J. Sietsma, "The glass transition as a free volume related kinetic phenomenon," *Acta Metallurgica Et Materialia*, vol. 38, no. 3, pp. 383–389, 1990.

[42] J. Li, F. Spaepen, and T. C. Hufnagel, "Nanometre-scale defects in shear bands in a metallic glass," *Philosophical Magazine A*, vol. 82, no. 13, pp. 2623–2630, 2002.

[43] B. P. Kanungo, S. C. Glade, P. Asoka-Kumar, and K. M. Flores, "Characterization of free volume changes associated with shear band formation in Zr- and Cu-based bulk metallic glasses," *Intermetallics*, vol. 12, no. 10-11, pp. 1073–1080, 2004.

[44] K. Hajlaoui, T. Benameur, G. Vaughan, and A. R. Yavari, "Thermal expansion and indentation-induced free volume in Zr-based metallic glasses measured by real-time diffraction using synchrotron radiation," *Scripta Materialia*, vol. 51, no. 9, pp. 843–848, 2004.

[45] A. R. Yavari, A. L. Moulec, A. Inoue et al., "Excess free volume in metallic glasses measured by X-ray diffraction," *Acta Materialia*, vol. 53, no. 6, pp. 1611–1619, 2005.

[46] K. Georgarakis, A. R. Yavari, D. V. Louzguine-Luzgin et al., "Atomic structure of Zr-Cu glassy alloys and detection of deviations from ideal solution behavior with Al addition by x-ray diffraction using synchrotron light in transmission," *Applied Physics Letters*, vol. 94, no. 19, Article ID 191912, 2009.

[47] X. D. Wang, J. Bednarcik, K. Saksl, H. Franz, Q. P. Cao, and J. Z. Jiang, "Tensile behavior of bulk metallic glasses by in situ x-ray diffraction," *Applied Physics Letters*, vol. 91, no. 8, Article ID 081913, 2007.

[48] J. J. Lewandowski and A. L. Greer, "Temperature rise at shear bands in metallic glasses," *Nature Materials*, vol. 5, no. 1, pp. 15–18, 2006.

[49] K. Georgarakis, M. Aljerf, Y. Li et al., "Shear band melting and serrated flow in metallic glasses," *Applied Physics Letters*, vol. 93, no. 3, Article ID 031907, 2008.

[50] W. J. Wright, R. B. Schwarz, and W. D. Nix, "Localized heating during serrated plastic flow in bulk metallic glasses," *Materials Science and Engineering A*, vol. 319–321, pp. 229–232, 2001.

[51] A. Van Den Beukel and S. Radelaar, "On the kinetics of structural relaxation in metallic glasses," *Acta Metallurgica*, vol. 31, no. 3, pp. 419–427, 1983.

[52] P. de Hey, J. Sietsma, and A. Van Den Beukel, "Structural disordering in amorphous $Pd_{40}Ni_{40}P_{20}$ induced by high temperature deformation," *Acta Materialia*, vol. 46, no. 16, pp. 5873–5882, 1998.

[53] H. M. Chen, J. C. Huang, S. X. Song, T. G. Nieh, and J. S. C. Jang, "Flow serration and shear-band propagation in bulk metallic glasses," *Applied Physics Letters*, vol. 94, no. 14, Article ID 141914, 2009.

[54] I. M. Krieger and T. J. Dougherty, "A mechanism for non-Newtonian flow in suspensions of rigid spheres," *Transactions of the Society of Rheology*, vol. 3, pp. 137–152, 1959.

[55] N. K. Halder, B. K. Chatterjee, and S. C. Roy, "The change of viscosity with concentration of suspended particles and a new concept of gelation," *Journal of Physics Condensed Matter*, vol. 9, no. 42, pp. 8873–8878, 1997.

[56] S. Wright, L. Zhang, S. Sun, and S. Jahanshahi, "Viscosity of a CaO-MgO-Al_2O_3-SiO_2 melt containing spinel particles at 1646 K," *Metallurgical and Materials Transactions B*, vol. 31, no. 1, pp. 97–104, 2000.

[57] H. J. Chang, D. H. Kim, Y. M. Kim, Y. J. Kim, and K. Chattopadhyay, "On the origin of nanocrystals in the shear band in a quasicrystal forming bulk metallic glass $Ti_{40}Zr_{29}Cu_9Ni_8Be_{14}$," *Scripta Materialia*, vol. 55, no. 6, pp. 509–512, 2006.

[58] M. Avrami, "Kinetics of phase change. II Transformation-time relations for random distribution of nuclei," *The Journal of Chemical Physics*, vol. 8, no. 2, pp. 212–224, 1940.

[59] S. Yoon, G. Bae, Y. Xiong et al., "Strain-enhanced nanocrystallization of a CuNiTiZr bulk metallic glass coating by a kinetic spraying process," *Acta Materialia*, vol. 57, no. 20, pp. 6191–6199, 2009.

[60] Y. F. Deng, L. L. He, Q. S. Zhang, H. F. Zhang, and H. Q. Ye, "HRTEM analysis of nanocrystallization during uniaxial compression of a bulk metallic glass at room temperature," *Ultramicroscopy*, vol. 98, no. 2–4, pp. 201–208, 2004.

[61] D. T. A. Matthews, V. Ocelík, P. M. Bronsveld, and J. Th. M. De Hosson, "An electron microscopy appraisal of tensile fracture in metallic glasses," *Acta Materialia*, vol. 56, no. 8, pp. 1762–1773, 2008.

[62] H. E. Kissinger, "Reaction kinetics in differential thermal analysis," *Analytical Chemistry*, vol. 29, no. 11, pp. 1702–1706, 1957.

[63] T. Ozawa, "Kinetic analysis of derivative curves in thermal analysis," *Journal of Thermal Analysis*, vol. 2, no. 3, pp. 301–324, 1970.

[64] S. X. Song, H. Bei, J. Wadsworth, and T. G. Nieh, "Flow serration in a Zr-based bulk metallic glass in compression at low strain rates," *Intermetallics*, vol. 16, no. 6, pp. 813–818, 2008.